THE JOURNAL OF BIOLOGICAL CHEMISTRY VOL. 282, NO. 37, pp. 26775–26785, September 14, 2007

Distinct Mechanisms for Ctr1-mediated Copper and Cisplatin Transport*

Received for publication, May 14, 2007, and in revised form, July 10, 2007 Published, JBC Papers in Press, July 12, 2007, DOI 10.1074/jbc.M703973200

Devis Sinani, David J. Adle, Heejeong Kim, and Jaekwon Lee[1]

From the Redox Biology Center, Department of Biochemistry, University of Nebraska, Lincoln, Nebraska 68588-0664

The Ctr1 family of integral membrane proteins is necessary for high affinity copper uptake in eukaryotes. Ctr1 is also involved in cellular accumulation of cisplatin, a platinum-based anticancer drug. Although the physiological role of Ctr1 has been revealed, the mechanism of action of Ctr1 remains to be elucidated. To gain a better understanding of Ctr1-mediated copper and cisplatin transport, we have monitored molecular dynamics and transport activities of yeast *Saccharomyces cerevisiae* Ctr1 and its mutant alleles. Co-expression of functional Ctr1 monomers fused with either cyan or yellow fluorescent protein resulted in fluorescence resonance energy transfer (FRET), which is consistent with multimer assembly of Ctr1. Copper near the K_m value of Ctr1 enhanced FRET in a manner that correlated with cellular copper transport. *In vitro* cross-linking of Ctr1 confirmed that copper-induced FRET reflects conformational changes within pre-existing Ctr1 complexes. FRET assays in membrane-disrupted cells and protein extracts showed that intact cell structure is necessary for Ctr1 activity. Despite Ctr1-dependent cellular accumulation, cisplatin did not change Ctr1 FRET nor did it attenuate copper-induced FRET. A Ctr1 allele defective in copper transport enhanced cellular cisplatin accumulation. N-terminal methionine-rich motifs that are dispensable for copper transport play a critical role for cisplatin uptake. Taken together, our data reveal functional roles for structural remodeling of the Ctr1 multimeric complex in copper transport and suggest distinct mechanisms employed by Ctr1 for copper and cisplatin transport.

Copper is a vital micronutrient required for the normal growth and development of many organisms from bacteria to humans (1). Copper mediates electron transfer reactions by virtue of its ability to donate or accept electrons through redox reactions (1). Thus, copper can serve as a cofactor for enzymes involved in a variety of essential physiological processes, including respiration, free radical detoxification, neurotransmission, iron metabolism, and signaling (1, 2). However, copper can readily catalyze reactions, which result in the production of toxic hydroxyl radicals (3, 4). The essential yet toxic nature of copper has been underscored by copper-related disorders in humans and animals. Nutritional copper deficiency leads to defects in growth and development (1, 2). Menkes and Wilson diseases are characterized by symptoms resulting from copper deficiency and excess accumulation, respectively (5–7). Several multifactorial degenerative disorders, such as Alzheimer disease and prion diseases, are also linked to imbalances in copper metabolism (8–10).

Delicate mechanisms for uptake, distribution, storage, and excretion of copper are involved in homeostatic copper metabolism. The baker's yeast *Saccharomyces cerevisiae* has been a useful model for the characterization of molecular mechanisms of copper metabolism in eukaryotes, because the structure and function for most of the molecular components involved in homeostatic metabolism of copper in yeast are conserved in other eukaryotes, including humans (2, 11–15). Extracellular copper exists in its oxidized form and is reduced by cell surface metalloreductases prior to transport (16). Reduced copper appears to be the substrate of Ctr1-mediated copper uptake with a K_m of 1~5 μM copper (17, 18, 31, 37). Ctr1 family members have been identified from a variety of eukaryotes such as yeast, plants, fruit fly, lizard, and mammals (12). Characterization of yeast, mice, and human cell lines where the *Ctr1* gene is deleted or overexpressed have demonstrated that Ctr1 is a necessary factor in high affinity copper uptake and supplies copper for all known copper-dependent physiological processes (17, 18, 31, 33, 38–40). Once inside, chaperones such as Atx1 and CCS deliver copper to the secretory compartment and to the copper-containing superoxide dismutase, respectively (19–22). Several proteins, such as Cox17 and Sco1, are involved in copper insertion into cytochrome *c* oxidase (23–25). Copper sequestration is handled by metallothioneins, which chelate excess copper to protect organisms from copper toxicity (26, 27). Given that Ctr2 is a vacuolar copper exporter (28), the vacuole may also serve as a copper storage and detoxification organelle. The copper-dependent transcriptional regulation of genes encoding components of copper acquisition and detoxification, including *Ctr1* and metalloreductases, has been characterized in yeast (2, 12, 15, 26). In addition, copper can also trigger the internalization and degradation of Ctr1 in yeast and human cells (51, 52). These modes of regulation of Ctr1 may play important roles in maintaining optimal levels of copper. However, given that contrasting results have been reported as well (58, 59), the nature and physiological significance of post-translational regulation of Ctr1 has not been firmly established.

* This work was supported by National Institutes of Health (NIH) Grant P20-RR-17675 (project 3 to J. L.), NIH Grant DK79209 (to J. L.), a Nutricia Foundation pre-doctoral fellowship (to D. S.), and funds provided through the Hatch Act in the University of Nebraska Agricultural Research Division. The costs of publication of this article were defrayed in part by the payment of page charges. This article must therefore be hereby marked "*advertisement*" in accordance with 18 U.S.C. Section 1734 solely to indicate this fact.

[1] To whom correspondence should be addressed: Dept. of Biochemistry, University of Nebraska-Lincoln, N210 Beadle Center, Lincoln, NE 68588-0664. Tel.: 402-472-2658; Fax: 402-472-7842; E-mail: jlee7@unlnotes.unl.edu.

Recent studies have implicated a new role for Ctr1 in the cellular accumulation of the chemotherapeutic drug cisplatin[2] (*cis*-diamminedichloroplatinum(II)) and its analogues. Deletion of the yeast and mouse *Ctr1* results in increased cisplatin resistance and a decrease in cisplatin accumulation (60). Human ovarian carcinoma cell lines overexpressing Ctr1 exhibit an increase in cisplatin import (62). *ATP7A* and *ATP7B*, two copper efflux transporters, are also involved in cisplatin efflux (63–65). Although these observations suggest that cisplatin uptake and extrusion employs copper transporters, the mechanism by which Ctr1 transports the chemically distinct copper and cisplatin, is poorly understood.

Ctr1 family members are integral membrane proteins spanning three trans-membrane domains (12). Ctr1 proteins are unique in their amino acid sequences and structural features (12, 15), however site-directed mutagenesis and truncation of Ctr1 have identified several residues that play roles in multimer assembly and copper transport (36, 37, 55, 57). For example, the methionine-rich motifs, which reside at the extracellular surface of Ctr1 family members appear to be involved in enhancing the efficiency of copper transport (36). Three conserved methionine residues, one at the extracellular N terminus and two at the predicted second trans-membrane domain, have been proposed as copper binding residues during copper translocation (36) (Fig. 1*A*). Several lines of biochemical, genetic, and biophysical analyses indicate that Ctr1 multimerizes at the plasma membrane (31,33–36,54). A recent projection structure of human Ctr1 determined using two-dimensional cryoelectron crystallography further showed that human Ctr1 forms a compact trimer with a novel channel-like architecture rather than the structural design of active transporters (53). This feature of Ctr1 assembly suggests that copper is translocated through the pore formed at the center of the Ctr1 trimer complex. Alternatively, like other typical transporters Ctr1-mediated copper translocation may be coupled with structural remodeling in the Ctr1 multimeric complex. Because Ctr1 family members do not carry a domain that is implicated in ATP utilization as a source of energy (2, 17, 12, 31), the electrochemical gradient of free copper and/or other ions across the plasma membrane may be the driving force for Ctr1-mediated copper transport (31).

To gain better insights into the mechanisms of action of Ctr1, we monitored molecular events coupled with Ctr1 transport activities and measured cellular copper and cisplatin uptake in yeast *S. cerevisiae*. Co-expression of yeast Ctr1 monomers tagged with either cyan or yellow fluorescent protein at the cytoplasmic C terminus resulted in fluorescence resonance energy transfer (FRET) in yeast cells. Quantification of copper-induced FRET changes between Ctr1 monomers *in situ* and cross-linking and Western blot analysis of Ctr1 showed that copper induces conformational changes of the Ctr1 multimeric complex. Correlation of FRET changes in Ctr1 with cellular copper uptake revealed an implication of structural remodeling of Ctr1 in copper translocation, which suggests transporter-like activity of Ctr1. Measurement of cisplatin-induced Ctr1 FRET and cellular cisplatin accumulation by Ctr1 mutant alleles showed that the mechanism of cisplatin uptake differs from the one employed during copper uptake.

[2] The abbreviations used are: cisplatin, *cis*-diamminedichloroplatinum(II); BCS, bathocuproine disulfonic acid; ECFP, enhanced cyan fluorescent protein; EGS, ethyleneglycol bis(succinimidylsuccinate); EYFP, enhanced yellow fluorescent protein; FRET, fluorescence resonance energy transfer; PIPES, 1,4-piperazinediethanesulfonic acid; MES, 4-morpholineethanesulfonic acid; SC, synthetic complete; ICPMS, inductively coupled plasma mass spectrometry.

EXPERIMENTAL PROCEDURES

Strains, Media, and Growth Conditions—A BY4741 haploid *S. cerevisiae* strain (*MATa his3Δ1 leu2Δ0 met15Δ0 ura3Δ0*), in which *Ctr1* gene is knocked out (*ctr1*::*kanMX4*) and *Ctr3* gene is not expressed (Open Biosystems) (43), was used for the experiments. Yeast cells were cultured with synthetic complete (SC) media (2% dextrose, 0.2% amino acid mixture, and 0.67% yeast nitrogen base) lacking specific markers for plasmid selection or YPD (2% dextrose, 2% Bacto-peptone, 1% yeast extract) media. Solid media were prepared with the supplementation of 1.5% agar. SUCFM medium (51) (0.67% yeast nitrogen base minus copper (Bio 101), 0.08% amino acid mixture, 50 mM MES buffer, pH 6.1) was used for culturing cells at low copper growth conditions. Yeast cell growth on non-fermentable carbon source media was tested using YPEG media (2% Bacto-peptone, 1% yeast extract, 2% ethanol, 3% glycerol, 1.5% agar). Yeast cells were cultured at 30 °C, if no growth temperature is specified.

Plasmid Construction and Manipulation—Ctr1 and *Ctr3* coding sequence was amplified from yeast genomic DNA by PCR using gene-specific primer sets that are flanked by HindIII (5′-end) and XhoI (3′-end) sites. For the epitope tagging at the C terminus of Ctr1, an NotI restriction enzyme site was inserted in the reverse primer just before the stop codon. The HindIII- and XhoI-digested PCR product was cloned into the p415-TEF or p416-TEF yeast vector (44) for a constitutive *TEF* gene promoter-mediated expression of *Ctr1* and *Ctr3*. ECFP and EYFP coding sequences without start and stop codons were PCR-amplified from pECFP-C1 and pEYFP plasmids (BD Biosciences-Clontech), respectively, with gene-specific primer sets flanked by NotI sites. The ECFP and EYFP PCR products were inserted into the NotI site of Ctr1 cloned in p416-TEF and p415-TEF vectors, respectively. A *Ctr1* mutant allele carrying a site-directed mutation of the conserved methionine (Met-127) to alanine (M1) and a mutant allele with a deletion of all eight N terminus Met-rich motifs (Δ8) (36) (Fig. 1*A*) was inserted into the same vectors. ECFP or EYFP was fused at the C-terminal tail of the Ctr1 mutant alleles. All constructs were confirmed by sequencing. Common molecular biology techniques, including plasmid amplification using *Escherichia coli*, and purification, followed previously established methods (45). Plasmid transformation into yeast was performed using the lithium acetate method (46). Cells transformed with the p415-TEF and p416-TEF vectors were selected and maintained using SC media lacking leucine and uracil.

Functional Assays of Ctr1 Fused with ECFP and EYFP—The function of wild-type Ctr1 and Ctr1 fused with either ECFP or EYFP was determined by complementation studies in the BY4741 yeast strain carrying a *Ctr1* deletion (*ctr1*Δ). Briefly, BY4741 *ctr1*Δ cells expressing empty vector, wild-type Ctr1, or Ctr1 fused with ECFP and EYFP were grown to mid-log phase (A_{600} = 1.0) in SC-selective media. Cells (~5 μl) were spotted

on YPEG media containing non-fermentable carbon sources where BY4741 *ctr1*Δ cells are not able to grow due to a defect in copper-dependent cytochrome *c* oxidase activities. Growth of BY4741 *ctr1*Δ cells transformed with vectors expressing Ctr1 or ECFP- or EYFP-fused Ctr1 was compared.

Fluorescence Microscopy—BY4741 *ctr1*Δ cells expressing wild-type or ECFP-tagged and/or EYFP-tagged Ctr1 were grown in SC media lacking leucine and uracil to mid-log phase. Cells were visualized using a confocal microscope (Olympus FV500) to localize Ctr1-ECFP and Ctr1-EYFP and determine the FRET between Ctr1 monomers. Cells were excited at 433 nm and 500 nm to observe ECFP and EYFP, respectively. Emission signals of ECFP and EYFP were detected at 475 nm and 525 nm, respectively. Images were processed using Adobe Photoshop 8.0.

Quantification of FRET—A scanning fluorometer was used to quantify FRET from yeast cells (BY4741 *ctr1*Δ) co-expressing functional Ctr1 tagged with either EYFP or ECFP at the C terminus. The method for measuring FRET efficiency in yeast cells suspended in buffer using a scanning fluorometry has been previously described (47). Briefly, yeast cells cultured to mid-log phase in selective media were washed twice using PIPES buffer (50 mM, pH 6.0), and re-suspended in the same buffer to A_{600} 1.0 ($\sim 10^7$ cells/ml). Fluorescent emission spectra by the excitation of ECFP or EYFP were obtained using a scanning fluorometer (PerkinElmer Life Sciences LS50). Cells were excited at 433 nm (ECFP excitation), and the emission was recorded from 460 nm to 580 nm. The following factors were considered to calculate the FRET efficiency in cells expressing both Ctr1-ECFP and Ctr1-EYFP. First, the emission spectrum from cells expressing untagged Ctr1 was subtracted to eliminate signal coming from auto fluorescence. Second, the emission spectrum of cells expressing Ctr1-ECFP and Ctr1 upon excitation of ECFP at 433 nm was obtained. This spectrum was subtracted to eliminate emission resulting from excitation of ECFP. Third, the emission spectrum upon excitation of EYFP at 433 nm of cells expressing Ctr1-EYFP with untagged Ctr1 was subtracted, which eliminates EYFP emission resulting from direct excitation at 433 nm. The spectrum obtained after completing these three steps is the EYFP emission resulting from FRET. FRET efficiency was calculated by dividing the EYFP emission peak area resulting from FRET by the peak area of the EYFP emission resulting from direct excitation of EYFP at 500 nm. Excel and Igor Pro (version 5.0) programs were used for data processing and statistical analysis.

Metal-induced FRET—To measure copper-induced changes in FRET, copper ($CuCl_2$, 2.5–25 μM) was added to PIPES buffer (50 mM, pH 6.0) containing yeast cells. Cells were gently mixed with copper at room temperature for 0–45 s and were scanned with a fluorometer for 75 s (total incubation time, 75–120 s). To determine metal specificities and cisplatin effect on Ctr1 FRET, we applied several metal ions, including silver ($AgNO_3$), cobalt ($CoSO_4$), zinc ($ZnCl_2$), and cadmium ($CdCl_2$) purchased from Sigma, and cisplatin (American Pharmaceutical Partners Inc. and Sigma). Temperature dependence in copper-induced FRET was measured from cells preincubated at 0, 10, 25, and 30 °C for 15 min.

In Vitro FRET Assays—BY4741 ctr1Δ cells transformed with Ctr1-ECFP and/or Ctr1-EYFP expression plasmids were cultured in selective media to mid-log phase. Cells were washed with ice-cold water and suspended in lysis buffer (phosphate-buffered saline, pH 7.5) with protease inhibitor mixture (Complete Mini, Roche Applied Science). Cells were vortexed with acid-washed glass beads at full speed six times for 2 min and centrifuged at 1000 × *g* for 3 min. The supernatant was considered as a broken-cell fraction. To solubilize proteins, the samples were incubated with Triton X-100 (1% final concentration) for 30 min on ice, and centrifuged at 16,000 × *g* for 15 min. The supernatant containing total protein extract was collected. Plasma membrane-disrupted cells, and total protein extracts were suspended in PIPES buffer (50 mM, pH 6.0) at the concentration of 60 μg/ml. FRET efficiency in the samples was measured with or without copper supplementation by scanning fluorometry using the same method as described above.

Western Blot Analysis—Protein extracts were denatured in SDS sample buffer at 95 °C for 5 min, resolved by SDS-PAGE, and transferred to a nitrocellulose membrane. Ctr1-ECFP was detected by chemiluminescence using anti-GFP antibodies (1:2,000) that detects not only GFP but also ECFP and EYFP, followed by horseradish peroxidase-conjugated anti-rabbit IgG antibodies (1:8,000, Santa Cruz Biotechnology, Santa Cruz, CA). Phosphoglycerate kinase was detected as loading control by chemiluminescence using anti-phosphoglycerate kinase antibodies (1:4,000, Molecular Probes) followed by horseradish peroxidase-conjugated anti-mouse IgG antibodies (1:10,000, Amersham Biosciences).

Temperature-dependent ^{64}Cu Uptake Assays—Cells were cultured to mid-log phase in selective media, washed twice using PIPES buffer (50 mM, pH 6.0), and re-suspended in the same buffer to A_{600} 1.0 ($\sim 10^7$ cells/ml). Cells were preincubated at 0, 10, 25, and 30 °C for 15 min. Radioactive ^{64}Cu (specific activity of 15–30 mCi/μg $CuCl_2$, Mallinckrodt Institute of Radiology at Washington University, St. Louis) was added to 1 ml of cells to a final concentration of 15 μM, and cells were incubated for 105 s. Samples were quenched with ice-cold phosphate-buffered saline containing 10 mM EDTA, filtered, and washed twice. ^{64}Cu was quantified using a γ-counter (PerkinElmer Life Sciences 1470 Wizard). Values obtained from empty vector control cells were subtracted from the values of cells expressing Ctr1 and normalized to the cell number.

Measurement of Cellular Metal Levels—Yeast cells were cultured until mid-log phase, spun down, and resuspended in 50 mM PIPES buffer (pH 6.0). Cells were cultured with copper or cisplatin, washed two times in phosphate-buffered saline containing 10 mM EDTA and 1 mM diethydithiocarbamate. Cell pellets were dissolved in 70% nitric acid and subsequently diluted to 10% nitric acid. Total cellular metal levels were measured by inductively coupled plasma mass spectrometry (ICPMS).

Cisplatin Toxicity Assay—Yeast cells cultured to mid-log phase in selective media were washed twice using YPD media, and re-suspended in YPD to A_{600} 1.0 ($\sim 10^7$ cells/ml). Cells were cultured at 30 °C for 2 h with or without supplementation of cisplatin (0.5 mM) in the media. Cells were diluted and plated on YPD media. Plates were incubated at 30 °C, and colonies were counted after 2 days.

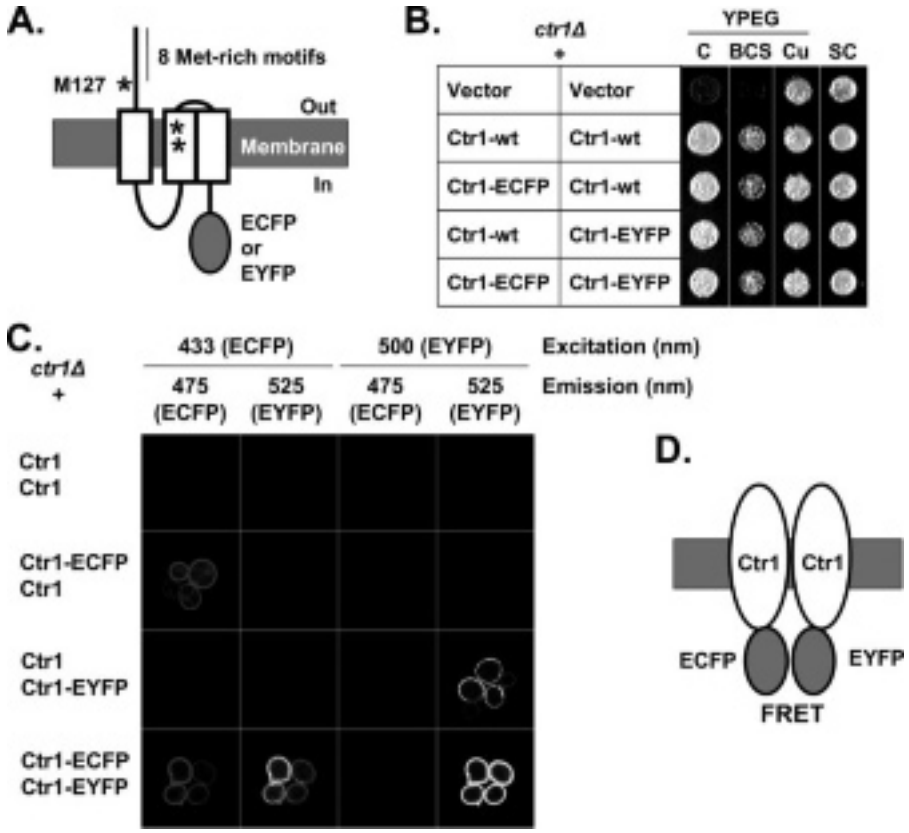

FIGURE 1. **Formation of functional oligomeric complexes by yeast Ctr1 monomers tagged with either ECFP or EYFP.** *A*, schematic depiction of yeast Ctr1 monomer fused with ECFP or EYFP at the cytosolic C terminus. The N-terminal extracellular region contains eight Met-rich motifs. The conserved Met-127 at the N terminus and two Met residues at the second transmembrane region are indicated (*). Three trans-membrane domains are shown as rectangles. *B*, co-expressed Ctr1 monomers, tagged with either ECFP or EYFP (Ctr1-ECFP or Ctr1-EYFP), are functional. *Ctr1* knock-out (*ctr1*Δ) cells were co-transformed with two plasmids for the constitutive expression of Ctr1 with or without fusion of ECFP or EYFP. Cells (5 μl of A_{600} = 0.1) cultured in synthetic complete media (SC) selecting for the two plasmids, were spotted on SC and non-fermentable (YPEG) growth media without (C) or with copper deficiency (100 μM BCS copper chelator supplementation to the media (YPEG plus BCS)) or copper addition (100 μM $CuCl_2$ (YPEG plus Cu)). Cells were grown at 30 °C for 3 days on YPEG media and for 1 day on SC media before photography. *C*, Ctr1 monomers fused with either ECFP or EYFP oligomerize. Cells were excited at 433 nm and 500 nm to visualize ECFP and EYFP, respectively. Emission signals of ECFP and EYFP were detected at 475 nm and 525 nm, respectively, using a confocal microscope. *D*, a model of the multimer assembly and FRET between Ctr1 monomers fused with ECFP or EYFP.

RESULTS

Ctr1 Multimer Formation in Situ—Yeast Ctr1 tagged at the C terminus with enhanced cyan or yellow fluorescent protein (Ctr1-ECFP or Ctr1-EYFP) (Fig. 1*A*) was constitutively expressed in *ctr1*Δ cells. The functionality of the tagged alleles was determined by complementation of the copper deficiency phenotype of yeast cells resulting from the defect of endogenous Ctr1 (Fig. 1*B*). Yeast cells lacking Ctr1 (*ctr1*Δ plus vector) cannot grow on YPEG media containing non-fermentable carbon sources such as ethanol and glycerol due to defects in the function of cytochrome *c* oxidase, a copper-requiring enzyme (Fig. 1*B*) (17). Yeast cells co-expressing untagged (Ctr1-wt) and ECFP or EYFP-tagged Ctr1 (Ctr1-ECFP or Ctr1-EYFP) did not exhibit any visible difference in growth on YPEG media and copper-deficient YPEG media supplemented with 100 μM BCS, a copper chelator (YPEG plus BCS) (Fig. 1*B*). The growth defect of *ctr1*Δ yeast cells was reversed on YPEG media supplemented with excess copper (100 μM $CuCl_2$) (YPEG plus Cu) and SC media containing a fermentable carbon source (glucose) lacking uracil and leucine (SC) for selection of the transformed plasmids. These results demonstrate that Ctr1 fused with ECFP or EYFP is fully functional.

We next examined Ctr1 multimer assembly *in situ* using a FRET approach. FRET relies on the distance-dependent (10–100 Å) non-radiative transfer of energy between donor and acceptor chromophores and is a powerful technique for studying molecular interactions (41, 42). Aliquots of yeast cells expressing combinations of untagged and chromophore-tagged Ctr1 (Ctr1/Ctr1, Ctr1-ECFP/Ctr1, Ctr1/Ctr1-EYFP, and Ctr1-ECFP/Ctr1-EYFP) were mounted on a glass slide and excited at 433 nm (ECFP excitation) and at 500 nm (EYFP excitation) using a confocal microscope. Emission signals for ECFP and EYFP were detected at 475 nm and 525 nm, respectively. ECFP and EYFP emission upon excitation with the corresponding wavelength is specific to cells expressing either ECFP or EYFP (Fig. 1*C*). Yeast cells expressing both Ctr1-ECFP and Ctr1-EYFP emit EYFP signal when ECFP is excited (Fig. 1*C*), suggesting Ctr1-ECFP and Ctr1-EYFP are close enough for FRET to occur (Fig. 1*D*). This is consistent with the formation of multimeric complexes of Ctr1 *in situ*. This FRET signal is specific between Ctr1 monomers, because cells co-expressing Ctr1-ECFP with Ctr3 C-terminally fused with EYFP (34) did not induce FRET (data not shown).

To confirm the FRET detected in microscopy and to efficiently quantify it, we measured the FRET signal using a scanning fluorometer. Cells expressing non-tagged Ctr1 (Ctr1 plus Ctr1), ECFP-tagged Ctr1 (Ctr1-ECFP plus Ctr1), EYFP-tagged Ctr1 (Ctr1 plus Ctr1-EYFP), and ECFP- and EYFP-tagged Ctr1 (Ctr1-ECFP plus Ctr1-EYFP) were grown overnight in selective media to mid log phase and suspended in PIPES buffer (50 mM, pH 6.0) to A_{600} 1.0 ($\sim 10^7$ cells/ml). Cells were excited at 433 nm (ECFP excitation) and emission was recorded from 460 to 580 nm (Fig. 2*A*). An emission peak for ECFP at 475 nm (single triangle) was observed from cells expressing Ctr1-ECFP and Ctr1 (*dotted line*) and Ctr1-ECFP and Ctr1-EYFP (*dashed dot line*). An emission peak for EYFP (*double triangle*) at 525 nm upon excitation of ECFP was observed from cells expressing Ctr1-ECFP and Ctr1-EYFP or Ctr1 and Ctr1-EYFP (*dashed line*). FRET was calculated as described under "Experimental Procedures" and is represented by the *solid line* (Fig. 2*A*). FRET between Ctr1 is consistent to the data published by another group (54) during preparation of this report. To better quantify

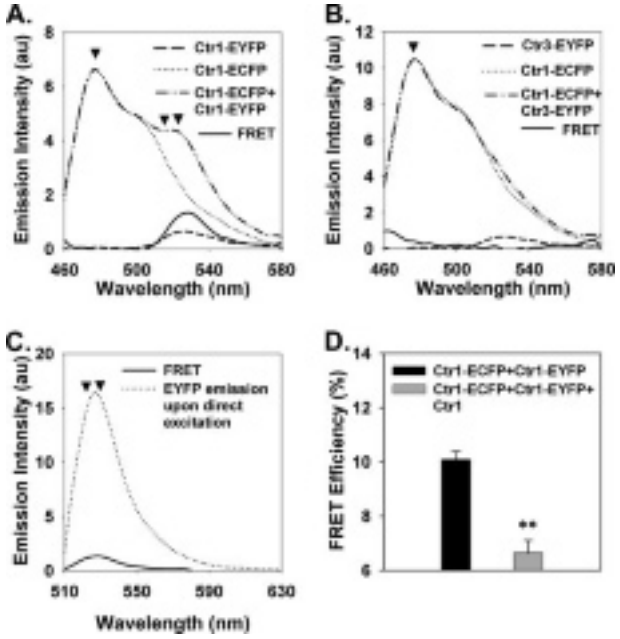

FIGURE 2. **Determination of FRET between Ctr1-ECFP and Ctr1-EYFP *in vivo* using a scanning fluorometer.** *A*, yeast cells expressing Ctr1 with or without fusion of ECFP or EYFP were excited at 433 nm (ECFP excitation), and the emission spectrum was recorded from 460 nm to 580 nm. ECFP (▼) and EYFP (▼▼) emission peaks are indicated. FRET data were analyzed as described under "Experimental Procedures." *B*, FRET experiments were performed on cells expressing Ctr1-ECFP and Ctr3-EYFP (*Ctr1-ECFP* + *Ctr3-EYFP*). *C*, determination of FRET efficiency. Cells expressing Ctr1-ECFP and Ctr1-EYFP (*Ctr1-ECFP* + *Ctr1-EYFP*) were excited at 500 nm (EYFP excitation) and the emission signal was recorded from 510 nm to 630 nm (dotted line). FRET was plotted on the same graph (*solid line*), and FRET efficiency was calculated by dividing the FRET peak area by the EYFP peak area. *D*, non-tagged Ctr1 was overexpressed in cells expressing Ctr1-ECFP and Ctr1-EYFP (*Ctr1-ECFP* + *Ctr1-EYFP* + *Ctr1*). The FRET efficiencies of cells expressing Ctr1-ECFP and Ctr1-EYFP (*black bar*) and of cells expressing Ctr1-ECFP and Ctr1-EYFP along with non-tagged Ctr1 (*gray bar*) were compared (* = $p < 0.001$, Student's *t* test). *A*, *B*, and *C* represent the average and *D* represents the average and standard deviation of four independent experiments.

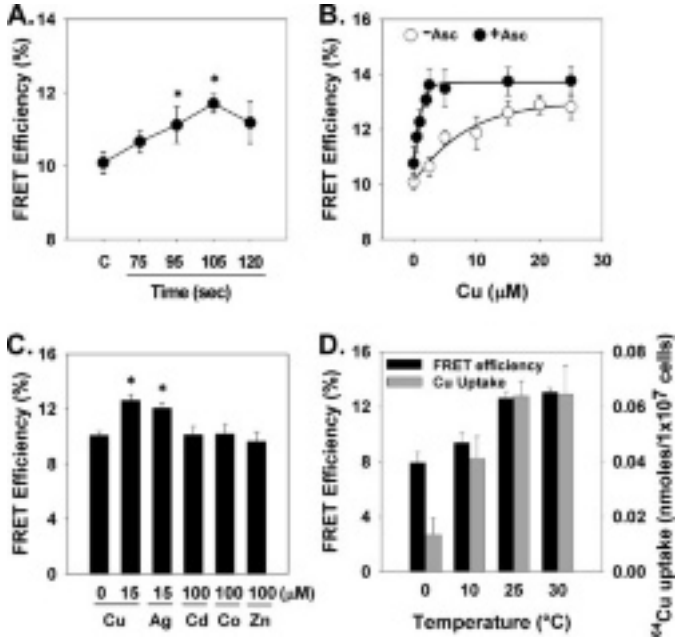

FIGURE 3. **Copper-induced changes in FRET efficiency between Ctr1-ECFP and Ctr1-EYFP.** *A*, time course of copper-induced FRET in Ctr1. Cells were cultured to exponential growth phase, washed, and re-suspended in PIPES buffer (50 mM, pH 6.0) to A_{600} 1.0. Copper (5 μM $CuCl_2$) was supplemented to the cell suspension, and FRET efficiency was calculated at different time points after the addition of copper (75–120 s, 0–45 s incubation and 75 s scanning) as described under "Experimental Procedures." *B*, copper dose response of Ctr1 FRET changes with or without ascorbate, a copper reductant. Copper ($CuCl_2$, 0.5–25 μM) was supplemented to the cell suspension for 30 s, and cells were scanned for 75 s. To reduce copper, $CuCl_2$ was preincubated with ascorbate (100 mM) for 1 h at room temperature and supplemented to cells suspended in PIPES buffer at the shown concentrations (0.1–25 μM). FRET efficiencies obtained with (*closed circle*) or without (*open circle*) addition of ascorbate were compared. *C*, metal specificity of Ctr1 FRET. $AgNO_3$ (*Ag*), $CoSO_4$ (*Co*), $CdCl_2$ (*Cd*), and $ZnCl_2$ (*Zn*) were applied to the cell suspension in the micromolar range, and cells were scanned with a fluorometer after addition of the metals. FRET efficiencies were calculated and compared. *D*, temperature dependence of Ctr1 FRET and ^{64}Cu uptake. Cells suspended in PIPES buffer were incubated at different temperatures (0, 10, 25, and 30 °C) for 15 min, prior to the addition of copper (15 μM at 105 s). Copper-dependent FRET and ^{64}Cu uptake were measured. FRET efficiencies (*black bars*) and ^{64}Cu levels (*gray bars*) were compared. Each data point represents average and standard deviation of at least four independent experiments. *, $p < 0.001$, Student's *t* test.

how efficiently ECFP emission excites EYFP through FRET, we calculated the FRET efficiency by dividing the peak area of the FRET emission by the peak area of the emission spectrum generated by exciting cells expressing Ctr1-ECFP and Ctr1-EYFP at 500 nm (EYFP excitation) (Fig. 2*C*). The FRET efficiency between Ctr1 monomers is 10.1 ± 0.3% (Fig. 3*D*, *black bar*). To determine whether this FRET signal was specific to interactions between Ctr1 monomers or whether it was due to nonspecific collisions between ECFP and EYFP at the plasma membrane, FRET was measured from cells co-expressing Ctr1-ECFP and Ctr3-EYFP, another trans-membrane protein, or cytosolic EYFP. No visible FRET signal was detected in cells co-expressing ECFP-tagged Ctr1 with either EYFP-tagged Ctr3 (Fig. 2*B*) or EYFP (data not shown). To further determine whether non-tagged Ctr1 competes for oligomerization with the tagged-Ctr1, we overexpressed non-tagged Ctr1 along with Ctr1-ECFP and Ctr1-EYFP. Indeed, non-tagged Ctr1 significantly reduced FRET efficiency to 6.6 ± 0.5% (Fig. 2*D*, *gray bar*). Taken together, these results demonstrate that FRET between Ctr1 monomers can be efficiently quantified in live yeast cells using a scanning fluorometer and that this signal is specific to Ctr1 monomer interactions *in situ*.

Copper Enhances FRET in Ctr1 Multimeric Complexes—To determine if the FRET signal produced in Ctr1 multimeric complexes is sensitive to copper, yeast cells co-expressing Ctr1-ECFP and Ctr1-EYFP were excited in the absence and presence of 5 μM copper. Because FRET efficiency correlates with the distance between the donor and the acceptor chromophores, the change in FRET efficiency in these complexes is indicative of the motion of Ctr1-ECFP and Ctr1-EYFP resulting in a change of the distance between ECFP and EYFP. Indeed, FRET between Ctr1-ECFP and Ctr1-EYFP was enhanced after the addition of copper (Fig. 3*A*). To determine time-dependent FRET response after copper exposure, cells were prepared as previously described and excited at different time points after the addition of 5 μM copper (75–120 s, 0–45 s incubation at 25 °C and 75 s scanning). The copper-induced FRET efficiency gradually increased and peaked close to 2 min before saturating (Fig. 3*A*). Because the scanning by the fluorometer requires 75 s, for short time point experiments (1–75 s), cells were fixed in paraformaldehyde (4%) under light-protection to minimize

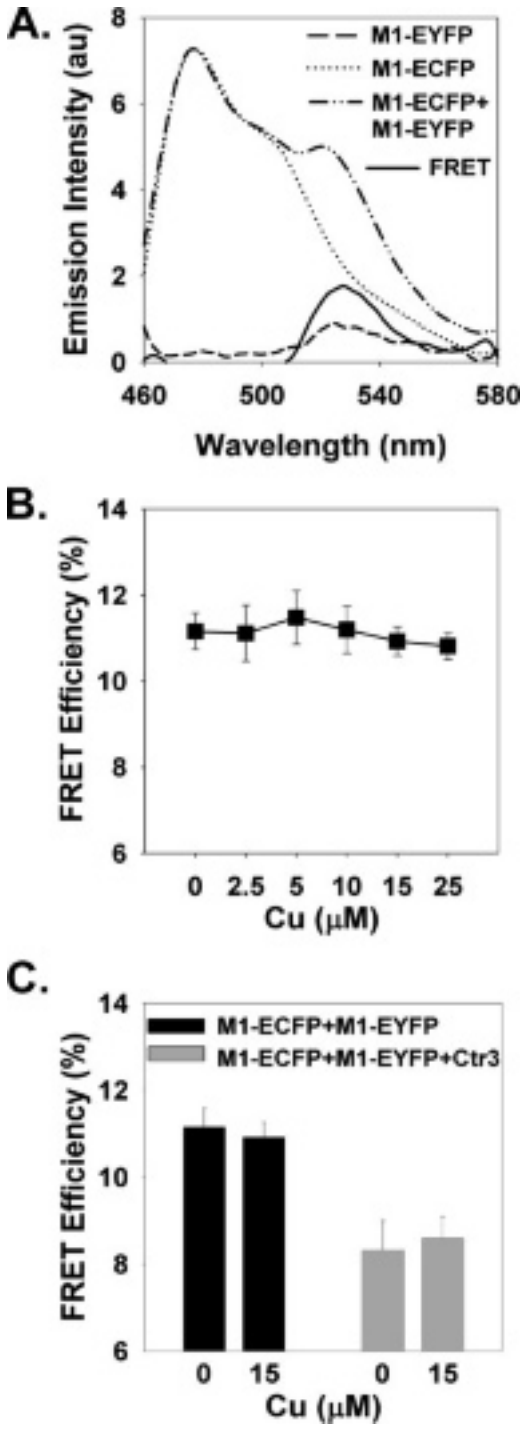

FIGURE 4. **Effect of copper on the FRET between non-functional Ctr1 monomers.** *A*, FRET was determined from cells transformed with two plasmids constitutively expressing non-functional M127A Ctr1 mutants (M1) with or without ECFP and/or EYFP fusion at the C terminus. *B*, copper-dependent FRET in the M127A mutant Ctr1. Copper ($CuCl_2$, 2.5 ~ 25 μM) was added to the yeast cells suspended in PIPES buffer for 30 s, and the cells were scanned for 75 s using a scanning fluorometer. FRET efficiencies as a function of copper concentrations were calculated as described under "Experimental Procedures" and compared. Each data point represents the average and standard deviation of four independent experiments. *C*, FRET was measured without or with copper (15 μM $CuCl_2$ for 30 s) supplementation on cells expressing functional Ctr3 along with the non-functional M1 mutant tagged with either ECFP or EYFP. FRET efficiencies were calculated (*gray bars*) and compared with the efficiencies of cells expressing only ECFP- and EYFP-tagged M1 (*black bars*).

bleaching of ECFP and EYFP, and then FRET was measured. Copper-induced FRET within 75 s was not statistically significant (data not shown). To measure the copper dose response of FRET, cells were scanned 30 s after the addition of various copper concentrations (2.5–25 μM). A copper-dependent FRET induction was observed in the range of the K_m of Ctr1 for copper, and FRET was saturated at higher copper concentrations (Fig. 3*B*, *open circle*). Because reduced copper rather than oxidized copper is believed to be a substrate for Ctr1 and the reduction is carried on by cell surface metalloreductases (16), we tested whether copper reduction is the limiting step of copper-induced FRET. Addition of copper preincubated with ascorbate (100 mM), a copper reductant, to the FRET assay buffer resulted in a dramatic increase in FRET efficiency (Fig. 3*B*, *closed circle*). We next measured FRET efficiency changes by other metal ions, including silver, cadmium, zinc, and cobalt, by adding micromolar ranges of these metals to the assay buffer. Among these metals only silver (15 μM), which shares similar chemical properties with reduced copper (48), exhibited a significant effect on Ctr1 FRET (Fig. 3*C*). These results further support the conclusion that FRET in Ctr1 is a copper-specific response. Because Ctr1-mediated copper transport is sensitive to temperature (31), we correlated copper-induced FRET with ^{64}Cu uptake at different temperatures (Fig. 3*D*). FRET efficiency and ^{64}Cu uptake were measured in cells suspended in PIPES (50 mM, pH 6.0) and incubated with 15 μM ^{64}Cu. The FRET efficiency was enhanced in a saturable fashion as the incubation temperature increased (Fig. 3*D*, *black bars*). ^{64}Cu uptake under the same experimental conditions correlated to FRET (Fig. 3*D*, *gray bars*). Consequently, copper-induced FRET in Ctr1 mirrored the characteristics of Ctr1-mediated copper uptake.

Defect in Copper-induced FRET in a Non-functional Ctr1 (M127A) Mutant—We next asked whether copper would have the same effect on FRET from a non-functional Ctr1 mutant. A Ctr1 mutant possessing a conserved extracellular methionine (Met-127) to alanine mutation (M1) (36) was fused with ECFP and/or EYFP. Two independent constructs were co-transformed in Ctr1 knock-out yeast cells. Expression and localization of the M1 mutant alleles is indistinguishable from that of wild-type Ctr1, but they are non-functional in copper transport (data not shown). FRET between the M1 mutants demonstrated that they form multimeric complexes (Fig. 4, *A* and *B*). However, no copper-induced FRET was observed in the M1 multimer at copper concentrations up to 25 μM (Fig. 4*B*). This further suggests that copper-induced FRET in Ctr1 is coupled with copper transport. To test whether the copper transported into the cytoplasm by other pathways induces Ctr1 FRET, we expressed Ctr3 along with the non-functional mutant M1 tagged with either ECFP or EYFP. Ctr3 is a Ctr1 family member in yeast that is functionally redundant to Ctr1, and our FRET assay between Ctr1 and Ctr3 showed that they do not physically interact *in vivo* (Fig. 2*B*). Ctr3 co-expressed with M1 mutants enhanced intracellular copper accumulation as determined by growth assay on copper-requiring media (data not shown). However, intracellular copper transported through Ctr3 did not lead to copper-dependent FRET changes between the M1 mutants (Fig. 4*C*), suggesting that copper-induced FRET in

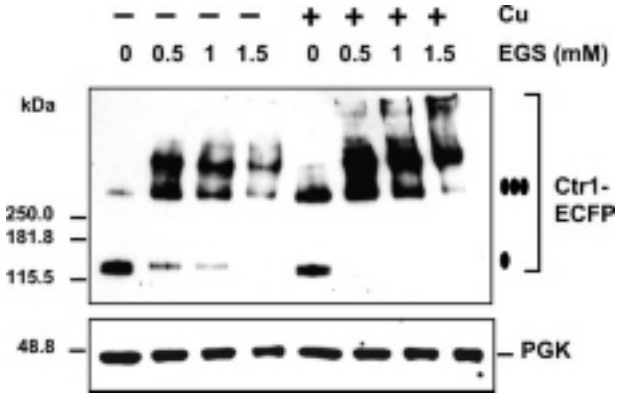

FIGURE 5. ***In vitro* cross-linking of the Ctr1 oligomeric complex to ascertain copper-dependent Ctr1 conformational changes.** *Ctr1* knock-out cells expressing Ctr1-ECFP and Ctr1-EYFP were cultured in synthetic complete media with or without copper supplementation (5 μM for 2 min). Total protein extracts were incubated with a primary amine cross-linker EGS at the shown concentrations and resolved by non-reducing SDS-PAGE. Ctr1 was detected by Western blot analysis with anti-GFP antibodies. Phosphoglycerate kinase (*PGK*) in the same samples was detected using anti-phosphoglycerate kinase antibodies as a control of specificity of Ctr1 cross-linking. Bands corresponding to the monomer and trimer species of Ctr1-ECFP are indicated with *one* and *three black ovals*, respectively.

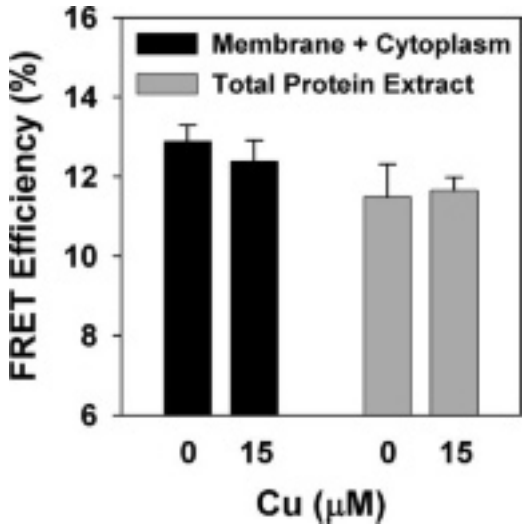

FIGURE 6. ***In vitro* FRET analyses.** Yeast cells expressing Ctr1 with or without fusion of ECFP or EYFP were vortexed with glass beads to perturb the membrane structure. Total proteins were extracted from the samples using Triton X-100 (1% final concentration). The broken cells (Membrane plus Cytoplasm, *black bars*) and protein extracts (*gray bars*) were re-suspended in PIPES buffer (60 μg/ml). Ctr1 FRET efficiency in the samples was measured using a scanning fluorometer in the presence or absence of copper (15 μM $CuCl_2$ for 30 s). Each data point represents the average and standard deviation of four independent experiments.

Ctr1 is coupled with the copper movement through the Ctr1 channel. Interestingly, Ctr3 co-expression reduced FRET in the M1 mutant multimers (Fig. 4*C*), possibly because Ctr3 may sequester other cellular component(s) that influence FRET in Ctr1.

Copper-induced FRET Changes in Ctr1 Occur as a Consequence of Conformational Changes in Pre-existing Ctr1 Complexes—We next examined copper-dependent Ctr1 structural changes using an *in vitro* protein cross-linking approach. Total protein extracts were prepared from yeast cells expressing Ctr1-ECFP cultured in media with or without copper (5 μM, 2 min) supplementation. The protein extracts were cross-linked using ethyleneglycol bis(succinimidylsuccinate) (EGS), which is a primary amine cross-linker and separated on SDS-PAGE. Ctr1-ECFP was detected by Western blot analysis using anti-GFP antibodies (Fig. 5). Increasing EGS concentrations shifted all the monomeric species of Ctr1 to the predicted homotrimer and higher oligomeric species suggesting that Ctr1 exists as a multimer in total protein extracts. Because phosphoglycerate kinase in the samples is detected as a monomeric species, the cross-linking is Ctr1 specific. Interestingly, cross-linking of Ctr1 to multimeric species was much more efficient in protein extracts prepared from copper-treated cells when compared with protein extracts from control cells (Fig. 5, *lane 2 versus lane 6*). Ctr1 in cells cultured with copper-supplemented media likely carries a distinct conformation that is more favorable for EGS cross-linking. Moreover, these data suggest that the copper-induced FRET (Fig. 3) must represent conformational changes, which occur in pre-existing multimer complexes rather than new multimer formation, because all of the Ctr1 exists as trimer and higher complexes in both control and copper-treated cells (Fig. 5, *lanes 4* and *8*).

In Vitro FRET Assays Showed That Proper Location of Ctr1 Is Necessary for Its Function—Copper uptake is not dependent on cellular ATP levels (31), but it appears that extracellular K^+ and acidic pH stimulate copper uptake (31, 50). Trans-membrane ionic gradients are known to be an important factor for several transport mechanisms, such as co-transport of proton and iron through DMT1 (DCT1 or Nramp2) divalent metal transporter (49). To examine the roles for transmembrane ionic gradient in Ctr1 activity, we measured Ctr1 FRET in membrane-disrupted cells and protein extracts from cells expressing ECFP or EYFP-fused Ctr1. The plasma membrane was perturbed by vortexing cells with glass beads as described under "Experimental Procedures." No live yeast cells remained under these conditions as confirmed by a cell growth assay on solid media (data not shown). Total protein extract was prepared by incubation of broken cells with 1% Triton X-100. The samples were suspended in PIPES buffer, and FRET was measured using a scanning fluorometer. FRET in broken cells and protein extracts was similar to that in intact cells (Fig. 6), suggesting that Ctr1 maintains a multimeric complex in these samples. However, copper did not enhance FRET (Fig. 6), suggesting no changes in the conformation of the Ctr1 multimer complex. To account for the possibility that copper reductases are not active under these experimental conditions, FRET induced by copper preincubated with ascorbate was measured. However, reduced copper again had no effect on Ctr1 FRET (data not shown). These data suggest that Ctr1 location at intact cell membranes is necessary for acquiring a driving force for conformational changes.

Cisplatin Does Not Induce Ctr1 FRET or Compete with Copper for FRET—Genetic and biochemical studies in yeast and mammalian cells have convincingly demonstrated that Ctr1 is a major factor for cellular accumulation of cisplatin (60–63, 66). However, it is still unclear whether Ctr1-mediated cisplatin accumulation employs the same mechanism used for copper uptake, particularly when considering the difference in structure and chemical properties between cisplatin and copper. Because copper enhanced Ctr1 FRET in a manner that corre-

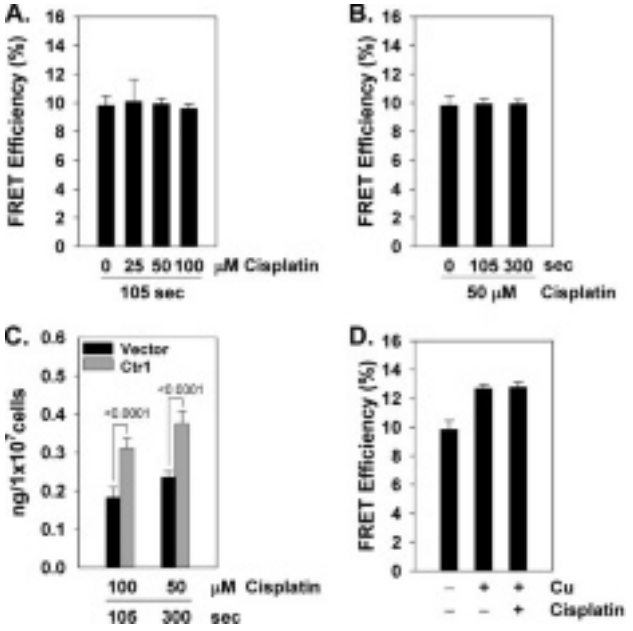

FIGURE 7. **Effect of cisplatin on the Ctr1 FRET and Ctr1-dependent cellular cisplatin accumulation.** *A*, cisplatin dose-response of Ctr1 FRET. Yeast cells expressing Ctr1 with or without fusion of ECFP or EYFP were cultured to exponential growth phase, washed, and re-suspended in PIPES buffer (50 mM, pH 6.0) to A_{600} 1.0. Cisplatin (25–100 μM) was supplemented to the cell suspension for 30 s and cells were scanned for 75 s. FRET efficiency was compared. *B*, time dependence of cisplatin-induced Ctr1 FRET. Cisplatin (50 μM) was supplemented to the cell suspension. Cells were scanned at 105 and 300 s after the addition of cisplatin (30 and 225 s incubation, respectively, and 75 s scanning). FRET efficiency was compared. *C*, cells treated with cisplatin under the same conditions as FRET were collected and washed, and cellular platinum levels were measured using ICPMS. *D*, effect of cisplatin on copper-enhanced Ctr1 FRET. FRET efficiencies were measured in cells re-suspended in PIPES buffer to A_{600} 1.0 with or without copper (15 μM) and cisplatin (100 μM). Data represent the average ± S.D. of four independent measurements. Statistical significance between data were compared by Student's *t* test as indicated.

lated with cellular copper uptake, we inquired whether cisplatin would have the same effect. Yeast cells co-expressing Ctr1-ECFP and Ctr1-EYFP were excited in the absence and presence of cisplatin. However, FRET between Ctr1-ECFP and Ctr1-EYFP was not changed after the addition of various concentrations of cisplatin (Fig. 7*A*) even after 5 min of exposure (Fig. 7*B*). To determine whether cells were accumulating cisplatin, platinum levels in cells were measured under the experimental condition used for FRET analysis. Cells were suspended in PIPES (50 mM, pH 6.0) and incubated either with 100 μM cisplatin for 105 s or 50 μM cisplatin for 300 s. Cell associated platinum was measured using ICPMS. Under both conditions cisplatin was at least one and a half times higher in cells expressing Ctr1 (Fig. 7*C*, *gray bars*) when compared with control cells expressing an empty vector (Fig. 7*C*, *black bars*), which shows that Ctr1 enhances cellular cisplatin levels despite no FRET change being observed. To determine whether cisplatin could attenuate the effect of copper on Ctr1 FRET through competition, we measured Ctr1 FRET in cells suspended in PIPES (50 mM, pH 6.0) and incubated with 15 μM copper in the presence or absence of 50 μM cisplatin (Fig. 7*D*). Copper enhancement of Ctr1 FRET efficiency was not significantly changed in the presence of excess cisplatin.

Cisplatin Accumulation and Toxicity in Cells Expressing Ctr1 Mutants—We next tested whether cisplatin could accumulate in cells expressing the Ctr1 (M127A) mutant (M1), which is defective in copper uptake (36) and does not display copper-enhanced FRET (Fig. 4*B*). *ctr1*Δ cells expressing either empty vector, Ctr1, or Ctr1(M127A) mutant (M1) were grown to mid-log phase resuspended in PIPES (50 mM, pH 6.0) and incubated with 15 μM copper or 50 μM cisplatin for 300 s. Cell-associated copper and cisplatin were measured using ICPMS. As expected the non-functional mutant M1 failed to accumulate copper (Fig. 8*A*). However, accumulation of platinum in cells expressing either Ctr1(M127A) or wild-type Ctr1 was similar to each other (Fig. 8*B*), suggesting that the Ctr1 mutant defective in copper uptake is able to enhance cellular cisplatin levels. Because it was proposed that cisplatin induces multimer stabilization of human Ctr1 through N-terminal methionine-rich motifs (67), we tested whether yeast cells expressing a Ctr1 allele with a deletion of all eight N terminus Met-rich motifs (Δ8) could accumulate cisplatin. In contrast to enhanced copper transport by the Δ8 mutant (Fig. 8*A*), no difference in cellular cisplatin accumulation was observed in cells expressing Δ8 when compared with cells expressing an empty vector (Fig. 8*B*). We next correlated cellular cisplatin accumulation with sensitivity to cisplatin. Because cells lacking Ctr1 or expressing the non-functional M1 allele are generally less healthy when compared with cells expressing a functional Ctr1, we co-expressed Ctr3 copper transporter in cells expressing vector, wild-type Ctr1, M1, or Δ8. Ctr3 does not affect cisplatin uptake (60). Cells were cultured in YPD media for 2 h with or without supplementation of 0.5 mM cisplatin, and plated on YPD media (60). After 2 days cell survival was measured as a percentage of colonies from cisplatin-treated cultures compared with colonies from controls. Consistent to the fact that Δ8 does not affect cellular cisplatin accumulation, yeast cells expressing Δ8 showed resistance to cisplatin when compared with cells expressing Ctr1 or M1 (Fig. 8*C*). These data suggest a critical role for the N-terminal Met-rich motifs, but not for the conserved Met-127, in Ctr1-mediated accumulation and toxicity of cisplatin.

DISCUSSION

Physiological roles of Ctr1 in both copper transport and cellular cisplatin accumulation have been established. However the mechanisms of action employed by Ctr1 during these processes remain poorly understood. Our data support the conclusion that Ctr1-mediated copper transport is coupled with structural rearrangements of Ctr1 mutimeric complexes. This suggests that Ctr1 possesses transporter activity rather than serving as a pore for copper translocation across the plasma membrane, even though it was shown that Ctr1 forms a structure similar to an ion channel and the transmembrane pore is not structurally occluded (53). Moreover, monitoring cisplatin-induced FRET and cellular cisplatin accumulation by mutant Ctr1 alleles revealed that the mechanism for Ctr1-mediated cisplatin transport is distinct from that of copper.

Although yeast Ctr1 possesses a relatively long (~127 amino acids) C-terminal tail compared with other family members (12), ECFP and EYFP independently fused at the end of the C terminus of Ctr1 are within a distance in which FRET can

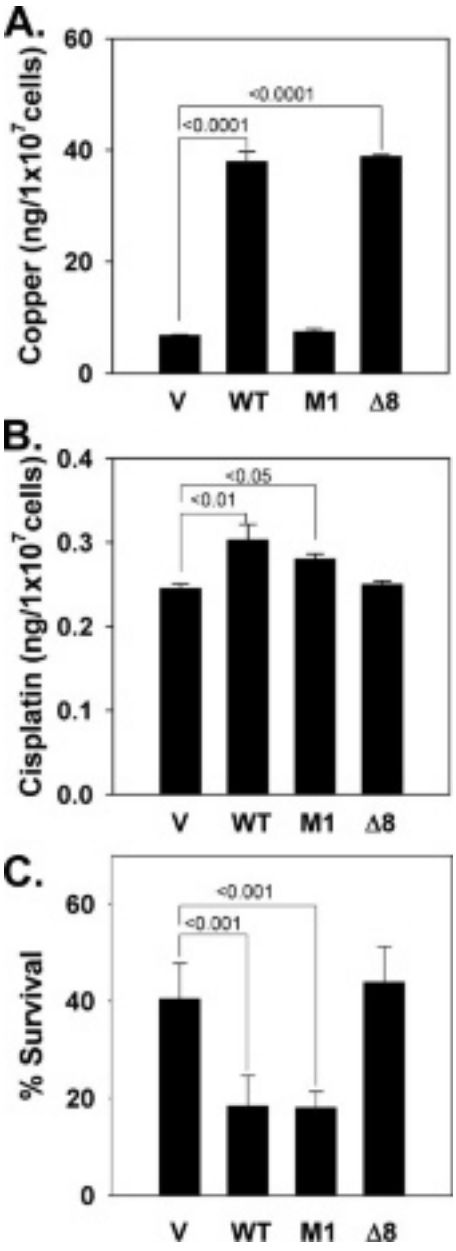

FIGURE 8. **Ctr1 mutant defective in copper uptake enhances cellular accumulation of cisplatin.** *A*, BY4741 *ctr1*Δ cells transformed with either empty vector (*V*), wild-type Ctr1 (*WT*), M127A Ctr1 (*M1*), or Ctr1 lacking all N-terminal eight Met-rich motifs (Δ*8*) were cultured in selective media to mid-log phase, resuspended in 50 mM PIPES (pH 6.0) and cultured with 15 μM copper at 30 °C for 5 min. Cells were collected and washed with PIPES buffer containing EDTA (10 mM), and cell-associated copper levels were measured by ICPMS. Data represent the average ± S.D. of four independent measurements. *B*, cells prepared as in *A*, were cultured with 50 μM cisplatin at 30 °C for 5 min. Cells were collected and washed with PIPES buffer containing cisplatin chelator diethydithiocarbamate (1 mM), and cell-associated platinum levels were measured by ICPMS. *C*, cisplatin sensitivity conferred by Ctr1 wild-type and mutants. BY4741 ctr1Δ cells expressing Ctr3 transformed with either empty vector (*V*), wild-type Ctr1 (*WT*), M127A Ctr1 (*M1*), or Ctr1 lacking all N-terminal eight Met-rich motifs (Δ*8*) expression construct. Cells grown in the plasmid selection media were re-suspended in YPD media (A_{600} 1.0) and were cultured at 30 °C for 2 h with or without 0.5 mM cisplatin supplementation. Cells were diluted and plated on YPD solid media. After incubating the plates at 30 °C for 2 days, growing colonies were counted. Data are expressed as percentages of colonies formed from cells exposed to cisplatin compared with colonies formed from control cells. Statistical significance between data were compared by Student's *t* test as indicated.

occur. This suggests that yeast Ctr1 is composed with at least two Ctr1 monomers *in situ*. Given that human Ctr1 forms a homotrimer (53), yeast Ctr1 likely forms a trimeric complex as well. However, our *in vitro* cross-linking and Western blot analysis of ECFP-fused Ctr1 interestingly showed not only a predicted trimer but also higher molecular weight complexes. It is possible that yeast Ctr1 may form a homo multimer complex higher than a trimer or associate with other proteins to form a functional copper transporter. Functional hetero and homo multimers have been observed in many transporters and ion channels. For example, P2X chloride channels and TRP channels are assembled by either homo or hetero multimerization of monomeric isoforms (68, 69). It is interesting to note that Ctr4 and Ctr5 two distinct Ctr1 homologues in *Schizosaccharomyces pombe* form a heteromultimeric complex, which is necessary for proper localization of each subunit to the plasma membrane and transporter activity (35). However, FRET analysis between Ctr1 and Ctr3 suggests that these Ctr1 family members do not form heteromultimers. Given that humans, plants, and fruit flies as well as yeast express more than one Ctr1 family proteins (12), the possibility of heteromultimer formation between Ctr1 family members in these species remains to be tested.

Quantification of FRET in a suspension of yeast cells using a scanning fluorometer is an efficient and powerful method for determining protein-protein interactions *in situ* and monitoring subtle and transient conformational changes associated with protein activities. Extracellular copper specifically enhanced FRET between ECFP- and EYFP-tagged Ctr1 monomers and intracellular copper transported by other pathways does not induce Ctr1 FRET. Thus, copper binding in the extracellular domain of Ctr1 must be transmitted through the transmembrane domains of Ctr1. Considering that FRET is proportional to the distance between the donor and acceptor (41, 42), enhanced FRET between ECFP and EYFP is a clear indication of motion of the cytosolic C termini leading to a shorter distance between the two fluorophores. Several lines of evidence presented in this study strongly suggest that copper-induced FRET is associated with Ctr1-mediated copper transport. First, the changes in FRET in response to copper correlate with the characteristics of Ctr1-mediated copper uptake. Second, the copper-induced FRET does not occur in a non-functional Ctr1 complex. This observation suggests that, despite the fact that Ctr1 forms a channel-like architecture carrying an unoccluded pore at the symmetric subunit interface (53), Ctr1 behaves like a transporter rather than a pore during copper transport. Although the homology in amino acid sequences of Ctr1 family members is not significant (12), biochemical and genetic analyses of the structure-function relations of yeast and human Ctr1 have suggested that the mode of action is conserved among Ctr1 family members (36). The conformational changes observed in yeast Ctr1 complexes likely occur in other Ctr1 family members, including human Ctr1. Consistently, it has been reported that the presence of copper during tryptic cleavage of human Ctr1 results in protection of the cytoplasmic loop between the predicted first and second transmembrane domains (37), which independently suggests copper-induced conformational changes in a Ctr1 family member.

Previous studies on Ctr1-mediated copper transport in a

mammalian cell line showed that proton and potassium levels in buffer or culture media affect Ctr1 activity (31), however the role of the transmembrane ionic gradient in Ctr1-mediated copper transport remains to be elucidated. Ctr1 in either membrane patches or protein extracts prepared using a buffer containing 1% Triton X-100 exhibited FRET, suggesting that Ctr1 still maintains a multimer complex under these conditions. However, copper did not induce FRET changes in Ctr1. Copper-induced structural changes in Ctr1 appear to require a specific environment maintained by live cells. A Ctr1 functional assay using purified Ctr1 or heterologous expression systems and structural characterization of Ctr1 *in vitro* may not reflect activity and structure of Ctr1 as expressed in its natural environment.

We propose that conformational changes in the Ctr1 multimeric complex play important roles in function and regulation of Ctr1. Copper binding to Ctr1 may initiate conformational changes that are transduced throughout the Ctr1 channel culminating with a motion of the C terminus tail when copper is released into the cytoplasm. Structure-function analysis of Ctr1 showed that three Met residues conserved throughout the Ctr1 family of proteins are necessary for Ctr1-mediated copper transport (36). These Met residues located at the extracellular N-terminal domain (~20 amino acids away from the first transmembrane domain) and the second transmembrane domain have been proposed as copper-binding residues (36). The three conserved methionines may serve as a selective filter for copper. Considering that Ctr1 forms a homotrimer, the external face of Ctr1 carries at least nine Met residues. However, no apparent copper binding residues, such as Met, Cys, and His, are conserved throughout the rest of the transmembrane region of Ctr1 family members. Thus, it is uncertain how copper moves from the periplasmic side to the cytoplasm and whether it is coordinated when it traverses the channel. Conformational rearrangement of the Ctr1 transmembrane domain induced by copper binding at the cell surface may be sufficient for removing the steric barrier(s) formed in the transmembrane pore. High-resolution snapshot structures of Ctr1 multimeric complexes in the copper-translocation cycle would further elucidate the dynamics of Ctr1 which we have observed in living cells. When copper reaches the cytoplasmic end of the pore, the cytoplasmic domains may coordinate copper and may be involved in its subsequent relay to cytoplasmic carriers. A few predicted copper binding residues, including at least one conserved cysteine residue, are present in these domains (data not shown). Because it has been shown that virtually no free copper exists in cells (70), it is reasonable to predict that interactions between intracellular copper chaperones and Ctr1 may be involved in efficient copper transport without releasing copper to the cytoplasm. FRET between Ctr1 and copper chaperones would be a useful approach for gaining further insights into molecular mechanisms of copper uptake across the plasma membrane. In addition, structural remodeling of Ctr1 may be implicated in regulation of its activity and expression at the cell surface. Copper-induced conformational changes in Ctr1 may expose regulatory domains or lead to formation of new domains, which attract other components of the copper uptake system. Because it was reported that Ctr1 in yeast and mammalian cells undergoes copper-induced endocytosis and degradation (51, 52), a specific conformation of Ctr1 resulting from excess copper exposure may recruit the machinery involved in the post-translational regulation of Ctr1.

An interesting dilemma about the structure and function of Ctr1 implicates the role of this transporter in the uptake of cisplatin, a widely used and effective cancer chemotherapy agent. Treatment failure is often associated with increased resistance to this drug. Cisplatin resistance has been ascribed to various mechanisms, including decreased accumulation, increased efflux, enhanced cellular detoxification, and DNA damage repair (71–73). Several previous reports suggest an implication of copper metabolism pathways in the uptake, chelation, and extrusion of cisplatin. Ctr1 is an important factor determining cellular cisplatin accumulation (60–62). Cisplatin can also induce expression of metallothionein, a chelator of copper and other metal ions (56, 76). Enhanced expression of copper efflux P-type ATPases has been observed in cisplatin-resistant cancer cells (63–65). However, the mechanistic basis of the implication of copper metabolic pathways in cisplatin metabolism remains uncertain. Our data clearly show that, despite Ctr1-dependent cellular accumulation, cisplatin did not affect Ctr1 FRET. Moreover, a Ctr1 mutant defective in copper uptake enhances cisplatin accumulation, whereas a copper transport-active Ctr1 mutant lacking all eight N terminus Met-rich motifs did not accumulate cisplatin. Together these data suggest that Ctr1 employs a different mechanism for copper and cisplatin transport and the rapid conformational changes in Ctr1 observed during copper translocation are not coupled with cisplatin uptake. The N-terminal Met-rich motifs seem to play a significant role for Ctr1-mediated cisplatin uptake. It is possible that binding of cisplatin to the N terminus of Ctr1 followed by subsequent internalization could be a mechanism for cisplatin uptake. The competition between copper and cisplatin in their uptake (60) may be due to internalization of Ctr1 by either copper and/or cisplatin, which would reduce the availability of Ctr1 at the cell surface thus reducing the uptake of either copper or cisplatin. However, copper- and cisplatin-induced internalization of Ctr1 (60, 74, 75) has been challenged by contrasting results indicating no effect of cisplatin on steady-state location of Ctr1 (58, 59, 67). Further elucidation of the mechanism of action and regulation of Ctr1 would lead to a better understanding of how Ctr1 can transport the essential mineral copper and the anticancer drug cisplatin and whether abnormal Ctr1 function and regulation is linked to the development of cisplatin resistance in cancer patients.

Acknowledgments—We thank Dr. Joe Zhou at the microscopy facility in the University of Nebraska-Lincoln for his assistance on confocal microscopy, Dr. Ted Huston at the University of Michigan for ICPMS, and Dr. Seiko Ishida at the University of California-San Francisco for cisplatin.

REFERENCES

1. Linder, M. C. (1991) *Biochemistry of Copper*, Plenum Press, New York
2. Pena, M. M., Lee, J., and Thiele, D. J. (1999) *J. Nutr.* **129,** 1251–1260
3. Halliwell, B., and Gutteridge, J. M. (1990) *Methods Enzymol.* **186,** 1–85
4. Uriu-Adams, J., and Yan Keen, C. L. (2005) *Mol. Aspects Med.* **26,**

268–298
5. Kaler, S. G. (1998) *Am. J. Clin. Nutr.* **67,** 1029S–1034S
6. Gitlin, J. D. (2003) *Gastroenterology* **125,** 1868–1877
7. Mercer, J. F. (2001) *Trends Mol. Med.* **7,** 64–69
8. Bush, A. I. (2003) *Trends Neurosci.* **26,** 207–214
9. Valentine, J. S., and Hart, P. J. (2003) Proc. *Natl. Acad. Sci. U. S. A.* **100,** 3617–3622
10. Cerpa, W., Varela-Nallar, L., Reyes, A. E., Minniti, A. N., and Inestrosa, N. C. (2005) *Mol. Aspects Med.* **26,** 405–420
11. Eide, D. J. (2000) *Adv. Microb. Physiol.* **43,** 1–38
12. Puig, S., and Thiele, D. J. (2002) *Curr. Opin. Chem. Biol.* **6,** 171–180
13. Van Ho, A., Ward, D. M., and Kaplan, J. (2002) *Annu. Rev. Microbiol.* **56,** 237–261
14. De Freitas, J., Wintz, H., Kim, J. H., Poynton, H., Fox, T., and Vulpe, C. (2003) *Biometals* **16,** 185–197
15. Lee, J., Adle, D., and Kim, H. (2006) in *Molecular Biology of Metal Homeostasis and Detoxification: From Microbes to Man (Topics in Current Genetics)* (M. Tamás and E. Martinoia, eds) Vol. 14, pp. 1–36, Springer-Verlag, Berlin Heidelberg
16. Hassett, R., and Kosman, D. J. (1995) *J. Biol. Chem.* **270,** 128–134
17. Dancis, A., Yuan, D. S., Haile, D., Askwith, C., Eide, D., Moehle, C., Kaplan, J., and Klausner, R. D. (1994) *Cell* **76,** 393–402
18. Knight, S. A., Labbe, S., Kwon, L. F., Kosman, D. J., and Thiele, D. J. (1996) *Genes Dev.* **10,** 1917–1929
19. Pufahl, R. A., Singer, C. P., Peariso, K. L., Lin, S.-J., Schmidt, P. J., Fahrni, C. J., Culotta, V. C., Penner-Hahn, J. E., and O'Halloran, T. V. (1997) *Science* **278,** 853–856
20. Yuan, D. S., Stearman, R., Dancis, A., Dunn, T., Beeler, T., and Klausner, R. D. (1995) *Proc. Natl. Acad. Sci. U. S. A.* **92,** 2632–2636
21. Culotta, V. C., Klomp, L. W. J., Strain, J., Casareno, R. L. B., Krems, B., and Gitlin, J. D. (1997) *J. Biol. Chem.* **272,** 23469–23472
22. Casareno, R. L., Waggoner, D., and Gitlin, J. D. (1998) *J. Biol. Chem.* **273,** 23625–23628
23. Glerum, D. M., Shtanko, A., and Tzagoloff, A. (1996) *J. Biol. Chem.* **271,** 14504–14509
24. Glerum, D. M., Shtanko, A., and Tzagoloff, A. (1996) *J. Biol. Chem.* **271,** 20531–20535
25. Carr, H. S., and Winge, D. R. (2003) *Acc. Chem. Res.* **36,** 309–316
26. Mehra, R. K., and Winge, D. R. (1991) J. *Cell. Biochem.* **45,** 30–40
27. Hamer, D. H. (1986) *Annu. Rev. Biochem.* **55,** 913–951
28. Rees, E. M., Lee, J., and Thiele, D. J. (2004) *J. Biol. Chem.* **279,** 54221–54229
29. Zhou, B., and Gitschier, J. (1997) *Proc. Natl. Acad. Sci. U. S. A.* **94,** 7481–7486
30. Lee, J., Prohaska, J. R., Dagenais, S. L., Glover, T. W., and Thiele, D. J. (2000) *Gene* (*Amst.*) **254,** 87–96
31. Lee, J., Pena, M. M., Nose, Y., and Thiele, D. J. (2002) *J. Biol. Chem.* **277,** 4380–4387
32. Jiang, J., Nadas, I. A., Kim, M. A., and Franz, K. J. (2005) *Inorg. Chem.* **44,** 9787–9794
33. Dancis, A., Haile, D., Yuan, D. S., and Klausner, R. D. (1994)) J. *Biol. Chem.* **269,** 25660–25667
34. Pena, M. M., Puig, S., and Thiele, D. J. (2000) *J. Biol. Chem.* **275,** 33244–33251
35. Zhou, H., and Thiele, D. J. (2001) *J. Biol. Chem.* **276,** 20529–20535
36. Puig, S., Lee, J., Lau, M., and Thiele, D. J. (2002) *J. Biol. Chem.* **277,** 26021–26030
37. Eisses, J. F., and Kaplan, J. H. (2002) *J. Biol. Chem.* **277,** 29162–29171
38. Lee, J., Prohaska, J. R., and Thiele, D. J. (2001) *Proc. Natl. Acad. Sci. U. S. A.* **98,** 6842–6847
39. Kuo, Y. M., Zhou, B., Cosco, D., and Gitschier, J. (2001) *Proc. Natl. Acad. Sci. U. S. A.* **98,** 6836–6841
40. Lee, J., Petris, M. J., and Thiele, D. J. (2002) *J. Biol. Chem.* **277,** 40253–40259
41. Selvin, P. R. (2000) *Nat. Struct. Biol.* **7,** 730–734
42. Sekar, R. B., and Periasamy, A. (2003) *J. Cell Biol.* **160,** 629–633
43. Winzeler, E. A., Shoemaker, D. D., Astromoff, A., Liang, H., Anderson, K., Andre, B., Bangham, R., Benito, R., Boeke, J. D., Bussey, H., Chu, A. M., Connelly, C., Davis, K., Dietrich, F., Dow, S. W., El Bakkoury, M., Foury, F., Friend, S. H., Gentalen, E., Giaever, G., Hegemann, J. H., Jones, T., Laub, M., Liao, H., Liebundguth, N., Lockhart, D. J., Lucau-Danila, A., Lussier, M., M'Rabet, N., Menard, P., Mittmann, M., Pai, C., Rebischung, C., Revuelta, J. L., Riles, L., Roberts, C. J., Ross-MacDonald, P., Scherens, B., Snyder, M., Sookhai-Mahadeo, S., Storms, R. K., Veronneau, S., Voet, M., Volckaert, G., Ward, T. R., Wysocki, R., Yen, G. S., Yu, K., Zimmermann, K., Philippsen, P., Johnston, M., and Davis, R. W. (1999) *Science* **285,** 901–906
44. Mumberg, D., Muller, R., and Funk, M. (1995) *Gene* (*Amst.*) **156,** 119–122
45. Ausubel, F. M., Brent, R., Kingston, R. E., Moore, D. D., Seidman J. G., Smith, J. A., and Struhl, K. (1987) *Current Protocol in Molecular Biology*, Wiley, New York
46. Gietz, R. D., Schiestl, R. H., Willems, A. R., and Woods, R. A. (1995) *Yeast* **11,** 355–360
47. Overton, M. C., and Blumer, K. J. (2002) *J. Biol. Chem.* **277,** 41463–41472
48. Zhu, Z., Labbe, S., Pena, M. M., and Thiele, D. J. (1998) *J. Biol. Chem.* **273,** 1277–1280
49. Gunshin, H., Mackenzie, B., Berger, U. V., Gunshin, Y., Romero, M. F., Boron, W.F., Nussberger, S., Gollan, J. L., and Hediger, M. A. (1997) *Nature* **388,** 482–488
50. De Rome, L., and Gadd, G. M. (1987) *FEMS Miocrobiol. Lett.* **43,** 283–287
51. Ooi, C. E., Rabinovich, E., Dancis, A., Bonifacino, J. S., and Klausner, R. D. (1996) *EMBO J.* **15,** 3515–3523
52. Petris, M. J., Smith, K., Lee, J., and Thiele, D. J. (2003) *J. Biol. Chem.* **278,** 9639–9646
53. Aller, S. G., and Unger, V. M. (2006) *Proc. Natl. Acad. Sci. U. S. A.* **103,** 3627–3632
54. Singh, A., Severance, S., Kaur, N., Wiltsie, W., and Kosman, D. J. (2006) *J. Biol. Chem.* **281,** 13355–13364
55. Aller, S. G., Eng, E. T., De Feo, C. J., and Unger, V. M. (2004) *J. Biol. Chem.* **279,** 53435–53441
56. Farnworth, P. G., Hillcoat, B. L., and Roos, I. A. (1989) *Chem.-Biol. Interact.* **69,** 319–332
57. Eisses, J. F., and Kaplan, J. H. (2005) *J. Biol. Chem.* **280,** 37159–37168
58. Klomp, A. E., Tops, B. B., Van Denberg, I. E., Berger, R., and Klomp, L. W. (2002) *Biochem. J.* **364,** 497–505
59. Eisses, J. F., Chi, Y., and Kaplan, J. H. (2005) *J. Biol. Chem.* **280,** 9635–9639
60. Ishida, S., Lee, J., Thiele, D. J., and Herskowitz, I. (2002) *Proc. Natl. Acad. Sci. U. S. A.* **99,** 14298–14302
61. Lin, X., Okuda, T., Holzer, A., and Howell, S. B. (2002) *Mol. Pharmacol.* **62,** 1154–1159
62. Holzer, A. K., Samimi, G., Katano, K., Naerdemann, W., Lin, X., Safaei, R., and Howell, S. B. (2004) *Mol. Pharmacol.* **66,** 817–823
63. Safaei, R., and Howell, S. B. (2005) *Crit. Rev. Oncol. Hematol.* **53,** 13–23
64. Komatsu, M., Sumizawa, T., Mutoh, M., Chen, Z. S., Terada, K., Furukawa, T., Yang, X. L., Gao, H., Miura, N., Sugiyama, T., and Akiyama, S. (2000) *Cancer Res.* **60,** 1312–1316
65. Samimi, G., Katano, K., Holzer, A. K., Safaei, R., and Howell, S. B. (2004) *Mol. Pharmacol.* **66,** 25–32
66. Raths, S., Rohrer, J., Crausaz, F., and Riezman, H. (1993) *J. Cell Biol.* **120,** 55–65
67. Guo, Y., Smith, K., and Petris, M. J. (2004) *J. Biol. Chem.* **279,** 46393–46399
68. North, R. A. (2002) *Physiol. Rev.* **82,** 1013–1067
69. Schaefer, M. (2005) *Pflugers Arch.* **451,** 35–42
70. Rae, T. D., Schmidt, P. J., Pufahl, R. A., Culotta, V. C., and O'Halloran, T. V. (1999) *Science* **284,** 805–808
71. Scanlon, K. J., Kashani-Sabet, M., Tone, T., and Funato, T. (1991) *Pharmacol. Ther.* **52,** 385–406
72. Giaccone, G. (2000) *Drugs* **59,** Suppl. 4, 9–17
73. O'Dwyer, P. J., Stevenson, J. P., and Johnson, S. W. (2000) *Drugs* **59,** Suppl. 4, 19–27
74. Holzer, A. K., Katano, K., Klomp, L. W., and Howell, S. B. (2004) *Clin. Cancer Res.* **10,** 6744–6749
75. Holzer, A. K., and Howell, S. B. (2006) *Cancer Res.* **66,** 10944–10952
76. Zelazowski, A. J., Garvey, J. S., and Hoeschele, J. D. (1984) *Arch. Biochem. Biophys.* **229,** 246–252